ACS Catalysis

pubs.acs.org/acscatalysis Research Article

Structural Diversification of Hapalindole and Fischerindole Natural Products via Cascade Biocatalysis

Robert M. Hohlman, Sean A. Newmister, Jacob N. Sanders, Yogan Khatri, Shasha Li, Nikki R. Keramati, Andrew N. Lowell, K. N. Houk, and David H. Sherman*

Cite This: *ACS Catal.* 2021, 11, 4670–4681 Read Online

ACCESS | Metrics & More | Article Recommendations | Supporting Information

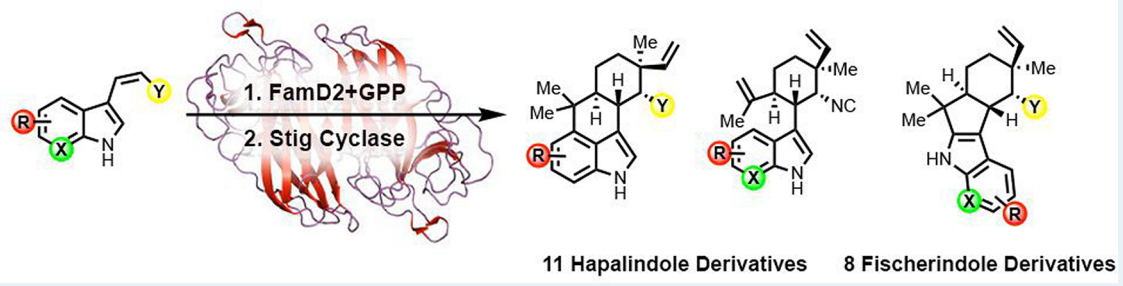

ABSTRACT: Hapalindoles and related compounds (ambiguines, fischerindoles, welwitindolinones) are a diverse class of indole alkaloid natural products. They are typically isolated from the Stigonematales order of cyanobacteria and possess a broad scope of biological activities. Recently the biosynthetic pathway for assembly of these metabolites has been elucidated. In order to generate the core ring system, L-tryptophan is converted into the *cis*-indole isonitrile subunit before being prenylated with geranyl pyrophosphate at the C-3 position. A class of cyclases (Stig) catalyzes a three-step process, including a Cope rearrangement, 6-*exo*-*trig* cyclization, and electrophilic aromatic substitution, to create a polycyclic core. The formation of the initial alkaloid is followed by diverse late-stage tailoring reactions mediated by additional biosynthetic enzymes to give rise to a wide array of structural variations observed in this compound class. Herein, we demonstrate the versatility and utility of the Fam prenyltransferase and Stig cyclases toward the core structural diversification of this family of indole alkaloids. Through the synthesis of *cis*-indole isonitrile subunit derivatives, and with the aid of protein engineering and computational analysis, we have employed cascade biocatalysis to generate a range of derivatives and gained insights into the basis for substrate flexibility in this system.

KEYWORDS: *Stig cyclase, Fam prenyltransferase, hapalindole, fischerindole, diversification, biocatalysis*

INTRODUCTION

Hapalindoles are a large family of indole alkaloids that have been isolated from the cyanobacterial order Stigonematales.[1] Along with their related compounds, fischerindoles, ambiguines, and welwitindolinones, there have been at least 81 members isolated from over 18 cyanobacterial strains.[2] They have also been shown to have antimicrobial,[3] antimycotic,[3e,4] anticancer,[5] and immunomodulatory activity.[6] Hapalindole/fischerindole metabolites possess three distinguishing features: a polycyclic ring system, diverse stereochemical variations, and the late-stage introduction of a range of functional groups such as additional rings, halogens, hydroxyls, isothiocyanate, and others. Due to these unique structural features and diverse biological activities, a number of total syntheses have been devoted to this family of indole alkaloids.[7] However, these efforts have been hindered due to the highly functionalized ring system and variant stereochemical patterns. Recently, work by several groups has explored the biogenesis of these metabolites,[8] which has uncovered new prenyltransferases, cyclases, halogenases, and other unique biosynthetic enzymes.

While each hapalindole subgroup has a characteristic ring connectivity and stereochemistry, current evidence indicates that they are all derived from a *cis*-indole isonitrile core combined with a geranyl monoterpene subunit. Through biosynthetic analysis, the mechanism for assembly of the hapalindole core was recently elucidated. L-Tryptophan is converted to *cis*-indole isonitrile precursor **1** by a three-enzyme cascade[8a] followed by geranylation at the C-3 position.[8f] In the presence of a Stig cyclase(s), this 3-geranyl *cis*-indole isonitrile (3-GC) intermediate **2** undergoes a Cope rearrangement, 6-*exo*-*trig* cyclization, and a terminal electrophilic aromatic substitution (EAS) at either the C-2 or C-4 indole position

Received: December 23, 2020
Revised: March 21, 2021
Published: April 5, 2021

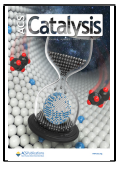

https://doi.org/10.1021/acscatal.0c05656
ACS Catal. 2021, 11, 4670–4681

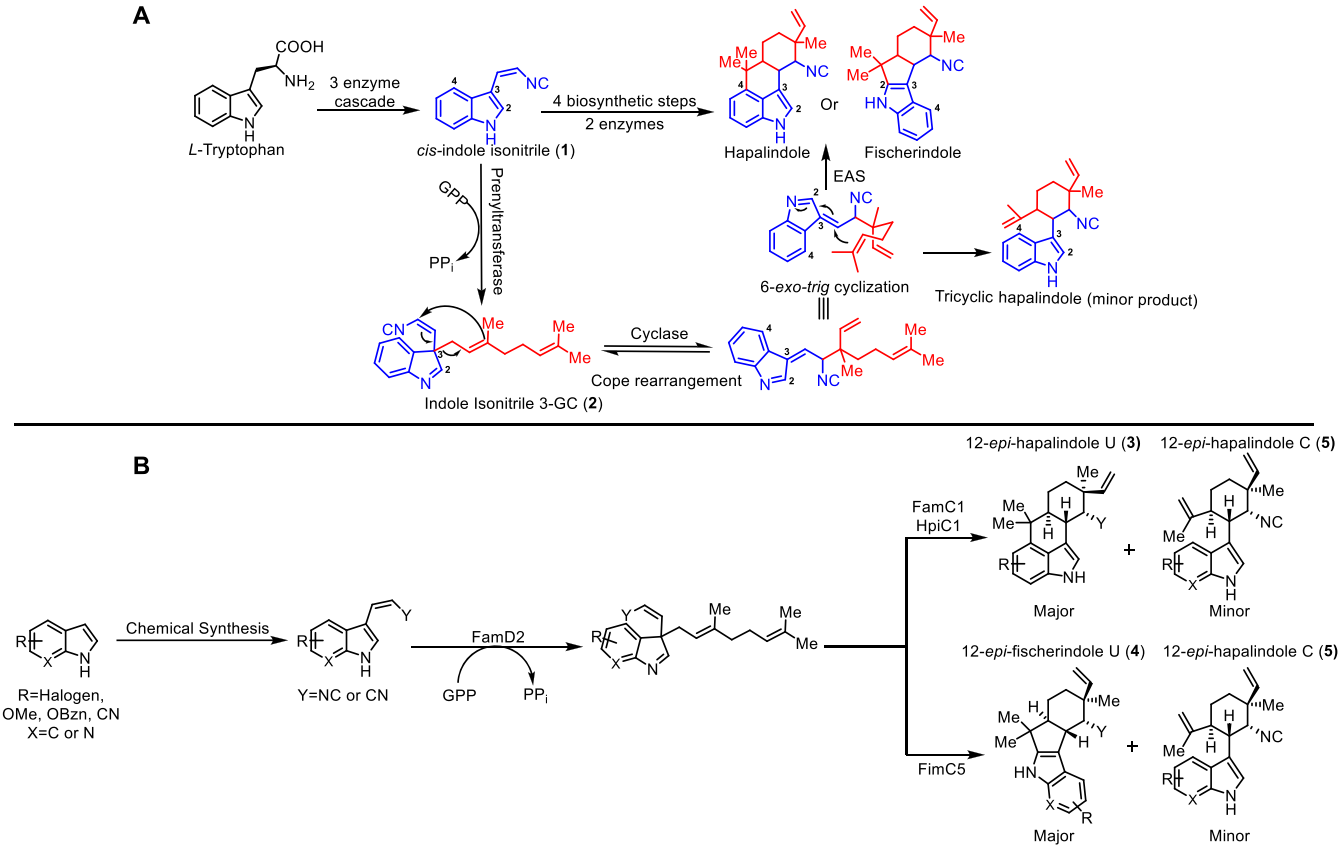

Figure 1. (A) Proposed biosynthesis of hapalindole type molecules. L-Tryptophan is converted into the *cis*-indole isonitrile core (**1**) (in blue) via a three-enzyme cascade followed by geranylation (in red) at the C-3 position to afford the 3-GC intermediate (**2**). In the presence of the cyclase(s), **2** undergoes a Cope rearrangement, 6-*exo*-*trig* cyclization, and electrophilic aromatic substitution (EAS) at the C-4 or C-2 position to afford the core hapalindole or fischerindole structure, respectively. (B) The approach described herein includes the chemical synthesis of unnatural *cis*-indole derivatives to show that the geranyltransferase (FamD2) and Stig cyclases can produce a range of unnatural 12-*epi*-hapalindole U (**3**), 12-*epi*-fischerindole U (**4**), and 12-*epi*-hapalindole C (**5**) compounds.

to afford the fischerindole or hapalindole core, respectively (Figure 1A).[8f] Subsequent late-stage tailoring of these molecules provides further access to the ambiguines and welwitindolinones.

Recently, cyanobacterial-derived Stig cyclases have attracted interest for their ability to catalyze a multistep core-forming cyclization cascade. Previous work has shown that the Stig cyclases exist in a dimeric state that may involve higher order oligomeric complexes to catalyze cyclization, including a terminal C−H functionalization reaction.[8h,p] Depending on the components of this oligomeric complex, different regio- and stereochemical outcomes have been observed.[8f,g,i,s,t] Structural and mutagenesis studies have revealed the key residues responsible for core hapalindole and fischerindole formation alongside computational analysis that has examined the cyclase-mediated Cope rearrangement and terminal EAS.[8h] Although gram-scale total syntheses of the hapalindoles have been achieved on a few select metabolites,[7o,t] further diversification is necessary for drug lead exploration. The Stig cyclases show potential as novel biocatalytic tools for developing unnatural hapalindole and fischerindole metabolites. Recently, we showed that fluorinated unnatural fischerindole and hapalindole derivatives could be produced using a microscale *in vitro* transcription/translation system with genes encoding prenyltransferase and Stig cyclase proteins.[9] To validate and explore this approach further, we demonstrate herein that key Stig cyclases can be employed as biocatalytic tools to produce numerous unnatural hapalindole and fischerindole compounds while also providing further mechanistic insights into the unusual cyclization cascade (Figure 1).

RESULTS AND DISCUSSION

Substrate Synthesis. To pursue our analysis, the chemical synthesis of unnatural *cis*-indole isonitrile derivatives was initiated. We synthesized these molecules via a Horner−Wadsworth−Emmons (HWE) olefination reaction from carboxyaldehyde indole derivatives on the basis of the ability to produce unnatural derivatives in a facile manner (Table 1). While the HWE reaction is known to stereochemically favor *trans*-(*E*) product formation, we found that performing the reaction at 0 °C yields a 50:50 ratio of the *cis*-(*Z*) and *trans* isomers. Using normal-phase chromatography, these isomers are readily separated to obtain the desired *Z*-isomer product. The majority of these derivatives were designed to have functional group modifications at the indole C-5 and C-6 positions, which included halogens (**10**−**16**), methoxy groups (**8**, **9**), benzyl groups (**6**), and a cyano (**7**) functionality. Two of the isomers (**17** and **18**) were modified at the C-7 position of the indole ring by replacement with a nitrogen atom. For derivatives **16** and **18**, the carboxyaldehyde indole precursor was commercially unavailable. Thus, we obtained the indole

https://doi.org/10.1021/acscatal.0c05656
ACS Catal. 2021, 11, 4670−4681

Table 1. *cis*-Indole Isonitrile Derivatives Generated in This Study and Isolated Percent Yield of the Desired *Z* Isomer

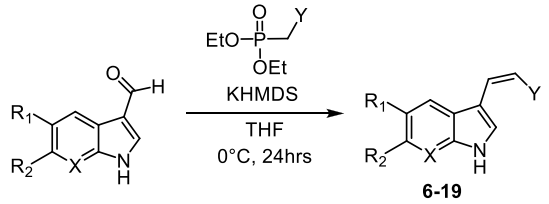

6-19

compound	substituent	yield of *Z* isomer (%)
6	R1 = OBzn, R2 = H, X = C,Y = NC	11
7	R1 = CN, R2 = H, X = C, Y = NC	22
8	R1 = OMe, R2 = H, X = C, Y = NC	16
9	R1 = H, R2 = OMe, X = C, Y = NC	5
10	R1 = Cl, R2 = H, X = C, Y = NC	11
11	R1 = H, R2 = Cl, X = C, Y = NC	16
12	R1 = F, R2 = H, X = C, Y = NC	18
13	R1 = H, R2 = F, X = C, Y = NC	23
14	R1 = Br, R2 = H, X = C, Y = NC	18
15	R1 = H, R2 = Br, X = C, Y = NC	23
16	R1 = I, R2 = H, X = C, Y = NC	18
17	R1 = H,R2 = H,X = N,Y = NC	13
18	R1 = F, R2 = H, X = N, Y = NC	18
19	R1 = H, R2 = H, X = C, Y = CN	16

precursor and added the carboxyaldehyde functionality via a Vilsmeier–Haack reaction that offered **20** and **21** (Experimental Section), allowing us to obtain derivatives **16** and **18**.

FamD2 Prenyltransferase. With a suite of *cis*-indole isonitrile derivatives in hand, we assessed the flexibility of FamD2 (also known as AmbP1), the prenyltransferase from *Fischerella ambigua* UTEX 1903,[8a,f] for the first key transformation of **1**. Through initial analytical reactions, we observed geranylation of 13 of the 14 substrates, with only the 5-cyano derivative **7** failing to be geranylated. This result was rationalized on the basis of previous structural studies of FamD2 that revealed conformational flexibility in the active site in the presence of a Mg^{2+} cofactor.[8n] In the case of **7**, we hypothesized that either steric hindrance or unfavorable electronics played a role in the lack of C-3 geranylation. Because substrate **16** (containing a large 5-iodo group) was able to be geranylated, we believed that steric hindrance was less likely to be a factor. Upon examination of the crystal structure of FamD2,[8n] we hypothesized that the highly polar 5-cyano functionality is interacting with a specific residue or the backbone of FamD2, disrupting the derivative from a favorable position for geranylation. Because the 3-GC intermediate has been shown to undergo a 1,2-shift,[8f] we sought a different method to analyze the efficiency of the geranylation step. Using an HPLC assay, total turnover numbers (TTN) were calculated over a 1 h reaction period at pH 10 to achieve maximum enzyme efficiency. Further cyclization reactions were conducted at pH 7 or 7.8, as the cyclase activity is greater under more acidic conditions.[8h,s] It is possible that FamD2 turnover is attenuated at a more neutral pH, but this was not tested. At pH 10, TTN values ranged from 710 to 1902, which highlights the versatility and efficiency of FamD2 as a biocatalyst over a range of unnatural substrates (Table 2).

FamC1 Cyclase. We next investigated the FamC1 cyclase from the *Fischerella ambigua* UTEX 1903 *fam* biosynthetic gene cluster. The homodimeric form of FamC1 produces 12-*epi*-hapalindole U[8f] and was previously shown to accept

Table 2. TTN Values for Geranylation Reaction with FamD2[a]

compound	TTN value
1	1495
6	1615
7	N/A[b]
8	1481
9	1902
10	947
11	1547
12	1625
13	803
14	755
15	1174
16	710
17	1281
18	1366
19	1454

[a]Assay conditions: 1 μM FamD2, 2 mM substrate, 1.5 mM GPP, 5 mM $MgCl_2$, 50 mM glycine (pH 10.0), 100 μL, 37 °C, 200 rpm, 1 h. [b]Compound **7** showed no conversion in the assay.

fluorinated *cis*-indole isonitrile derivatives **12** and **13** to generate the new hapalindole compounds **22** and **23**, respectively.[9] We sought to analyze and confirm its scope beyond fluorinated derivatives. Initially, few additional substrates showed conversion to the cyclized product. Lowering the pH and concentration of FamD2 did not increase the cyclase activity. As Ca^{2+} has been shown to be an important cyclase cofactor, we supplemented the reaction mixture to test its effect on FamC1 activity.[8g−i,s] Upon the addition of 5 mM calcium chloride, we observed increased production of cyclized products in 8 of the 14 unnatural substrates. On the basis of HPLC analysis, we estimated that the conversion values ranged from 10% to >99%. Scale-up efforts of 2 mg of each substrate enabled the structural characterization of these compounds. We confirmed that, in all but one case, the corresponding 12-*epi*-hapaplindole U derivative was produced. In contrast, FamC1 catalyzed the formation of tricyclic 12-*epi*-hapalindole C derivative **31** from azaindole compound **17** (Table 3). Tricyclic hapalindoles are normally a minor product observed in enzymatic reactions from previously studied Stig cyclases. We initially reasoned that the unnatural electronegative N-7 of the azaindole inhibited the terminal EAS reaction at the C-4 position. However, C-4 tetracycle formation was observed with the C-5-fluoro derivative **12**, which suggests that the selectivity may be guided by a skeletal variation of the N-7 position instead of the electronics of the indole ring.

HpiC1 Cyclase. While FamC1 demonstrated the ability to convert 8 of 14 substrates, we sought a cyclase with greater flexibility. We next examined HpiC1 from *Fischerella* sp. ATCC 43239, which shares an 84% sequence homology with FamC1. Complexes consisting of only HpiC1 have been shown to produce 12-*epi*-hapalindole U and trace levels of 12-*epi*-hapalindole C.[8g,h] A sequence comparison revealed only three active site variations between HpiC1 and FamC1.[8h] Analytical reactions showed an increased scope, as 10 of the 14 substrates were converted to hapalindole products with conversion values ranging from 30 to >99%. As with FamC1, the majority of the compounds were confirmed to be the corresponding 12-*epi*-hapalindole U derivatives. Similarly to reactions with FamC1,

https://doi.org/10.1021/acscatal.0c05656
ACS Catal. 2021, 11, 4670−4681

Table 3. Structures of 12-*epi*-Hapalindole U and 12-*epi*-Hapalindole C Derivatives Produced by FamC1 and HpiC1 from Unnatural *cis*-Indole Isonitrile or *cis*-Indole Nitrile Substrates[a]

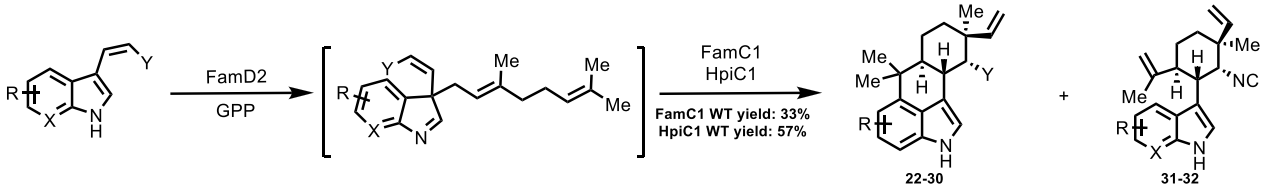

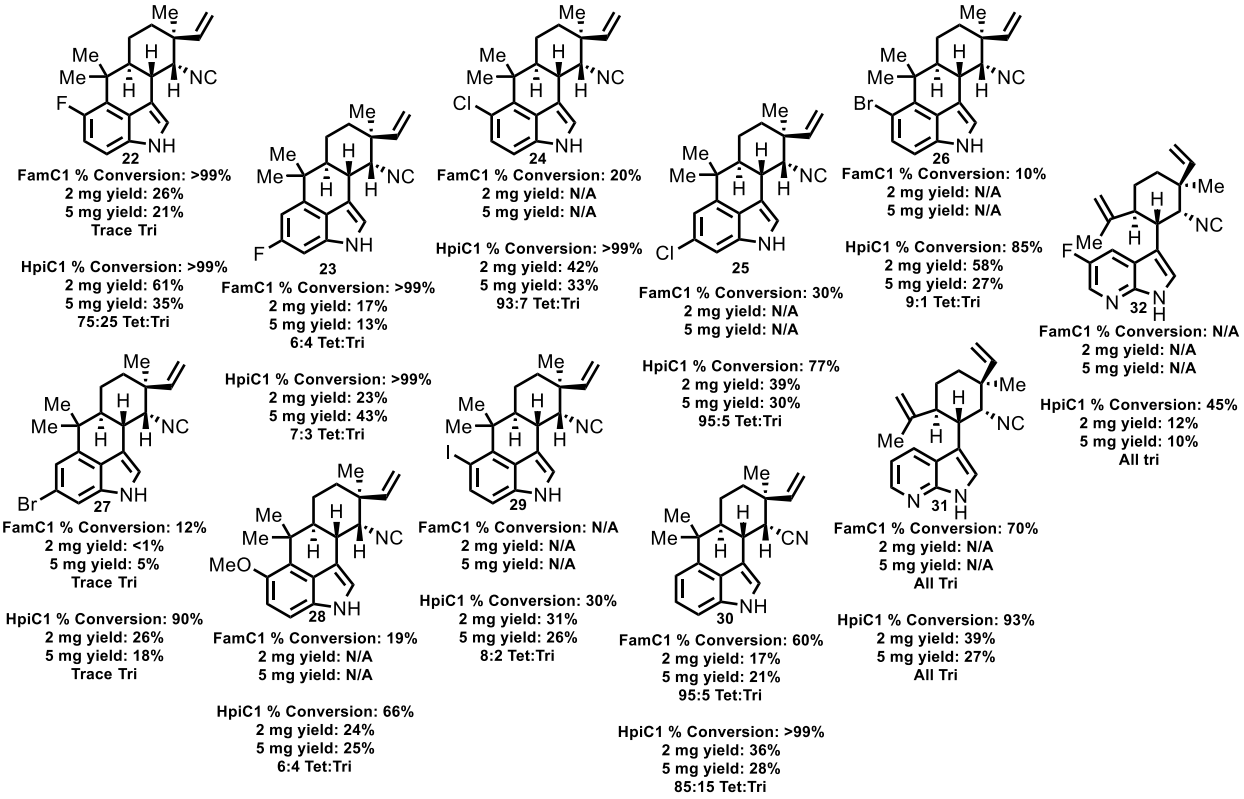

[a]Percent conversions, isolated yield values, and tetracyclic:tricyclic ratio (ratio estimated by NMR and/or HPLC) are shown below each derivative. N/A denotes that the derivative was either not produced by FamC1 or was not screened further in this study due to the enhanced versatility of HpiC1. HPLC conversion values were determined after 4 h in 100 μL reactions. Isolated yield values were determined from overnight reactions.

we observed the production of tricyclic 12-*epi*-hapalindole C derivatives **31** and **32** from *cis*-indole isonitrile substrates **17** and **18**, respectively (Table 3).

We hypothesized that the increased scope and reaction efficiency of HpiC1 could be attributed to the amino acid differences in the active site,[8h] resulting in less steric hindrance to accommodate larger substituents. We investigated the three amino acid differences in the active site between HpiC1 and FamC1 using site-directed mutagenesis to assess their role in the substrate scope, which are Val51, Phe138, and Leu147 in HpiC1. The HpiC1_V51I mutant revealed no changes in the substrate scope. Although single mutants (HpiC1_F138L and HpiC1_L147F) failed to show noticeable changes in scope, the percent conversions of substrates **8**, **14**, and **16** were reduced (Table S36 in the Supporting Information). The attenuated substrate scope of the double mutant (HpiC1_F138L_L147F) closely matched that of WT FamC1 (Figures S12−S22 in the Supporting Information). This mutagenesis study revealed that two of the three active site residue differences (138 and 147) were responsible for the change in substrate scope and conversion values between the two cyclases. Given that FamC1 exhibits low percent conversions for **14** and **15** and completely fails to convert **16**, we hypothesize that the two mutations present in HpiC1 (Phe138 and Leu147) reduce steric hindrance in the area of the active site that interacts with the C-5 and C-6 substituents of the indole, resulting in higher conversion efficiencies.

FimC5 Cyclase. Following an analysis of two hapalindole-producing cyclases, we explored FimC5, a fischerindole producing cyclase derived from *Fischerella muscicola* UTEX 1829. This cyclase produces 12-*epi*-fischerindole U[8g] and was used in our previous study to generate the two fluorinated derivatives **33** and **37**.[9] Analytical reactions showed the production of cyclized products for 8 of the 14 substrates tested with estimated conversion values ranging from 20% to >99%. The majority of the substrates were characterized as the corresponding 12-*epi*-fischerindole U derivatives. With substrate **17**, FimC5 catalyzed the formation of a 50:50 mixture of two products: the previously observed tricyclic derivative **31** and the new tetracyclic derivative **36**. The structural assignment of **36** was also confirmed using X-ray crystallography (Figure 2). In the case of derivative **18**, we only observed

https://doi.org/10.1021/acscatal.0c05656
ACS Catal. 2021, 11, 4670−4681

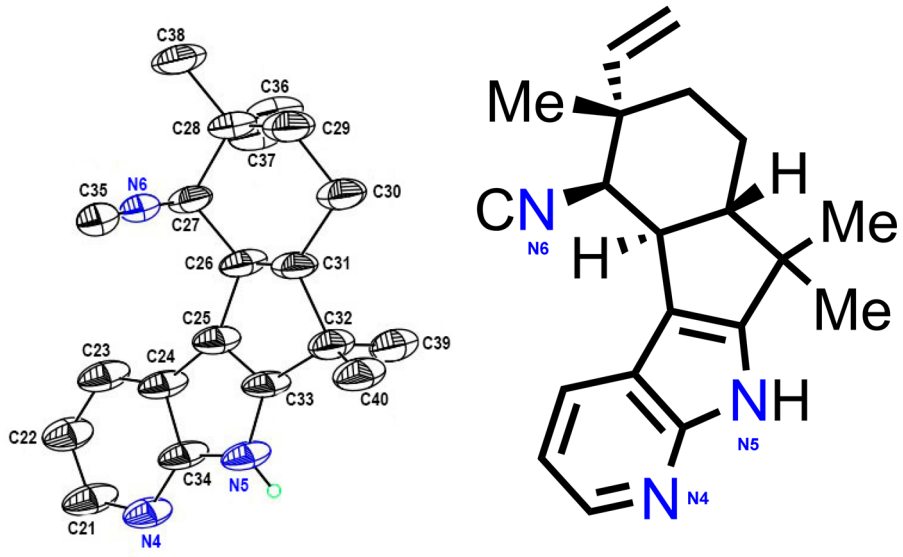

Figure 2. X-ray crystal structure of **36**. The NMR-assigned structure has been added to highlight the structural similarity. Nitrogen atoms have been highlighted in blue with same numbers to orient the reader.

Table 4. Structures of 12-*epi*-Fischerindole U Derivatives Produced by FimC5 from Unnatural *cis*-Indole Isonitrile or *cis*-Indole Nitrile Substrates[a]

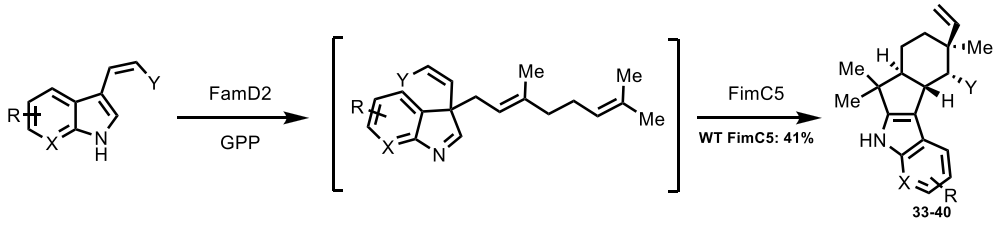

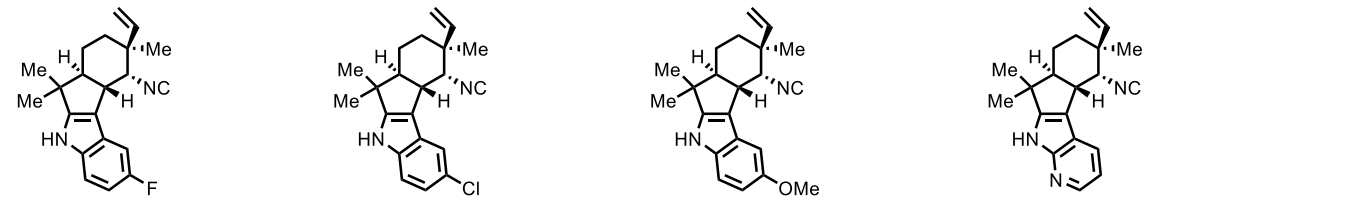

33
FimC5 % Conversion: >99%
2 mg yield: 32%
5 mg yield: 39%
All Tet

34
FimC5 % Conversion: 20%
2 mg yield: 18%
5 mg yield: 20%
85:15 Tet:Tri

35
FimC5 % Conversion: >99%
2 mg yield: 13%
5 mg yield: 11%
All Tet

36
FimC5 % Conversion: 98%
2 mg yield: 33%
5 mg yield: 32%
60:40 Tet:Tri

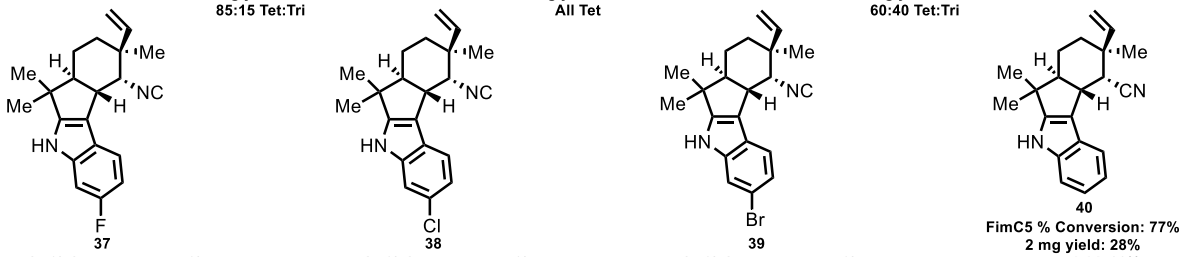

37
FimC5 % Conversion: >99%
2 mg yield: 29%
5 mg yield: 19%
All Tet

38
FimC5 % Conversion: 58%
2 mg yield: 24%
5 mg yield: 19%
85:15 Tet:Tri

39
FimC5 % Conversion: >99%
2 mg yield: 42%
5 mg yield: 26%
70:30 Tet:Tri

40
FimC5 % Conversion: 77%
2 mg yield: 28%
5 mg yield: 30%
All Tet

[a]Percent conversions, isolated yields, and tetracyclic:tricyclic ratio (ratio estimated by NMR and/or HPLC) are shown below each derivative. HPLC conversion values were determined after 4 h in 100 μL reactions. Isolated yield values were determined from overnight reactions.

production of the tricyclic derivative **32** (Table 4), with the C-5 fluorine appearing to limit reactivity at the C-2 position of the indole ring.

A previous analysis of FimC5 indicated that two active site amino acid residues (Phe101 and Ser138) play a key role in selectivity toward the indole C-2 or C-4 position for the terminal EAS.[8g,h] We decided to explore this further through site-directed mutagenesis with unnatural 3-GC derivatives. Three mutants of HpiC1 were produced to match the same residues identified in the FimC5 active site (Y101F, F138S,

https://doi.org/10.1021/acscatal.0c05656
ACS Catal. 2021, 11, 4670−4681

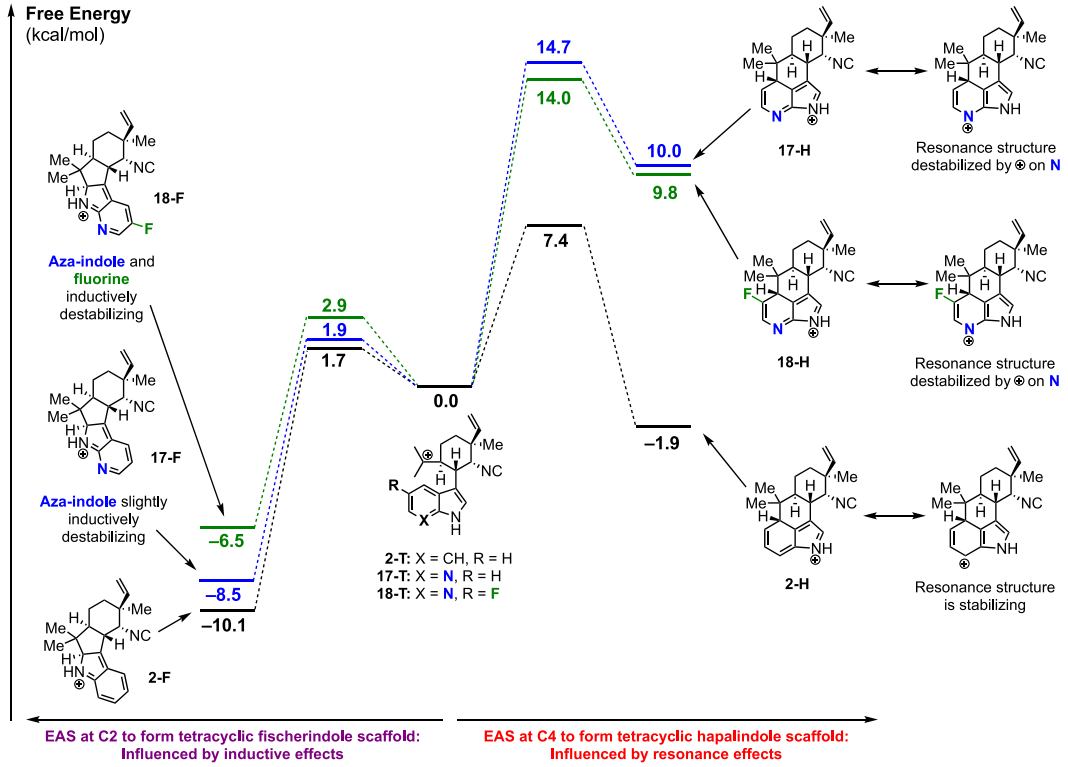

Figure 3. Quantum mechanical density functional theory computations comparing the energetics of tetracyclic hapalindole formation and tetracyclic fischerindole formation starting from the cationic intermediates derived from **2**, **17**, and **18**. The tetracyclic fischerindole formation (left side) is only influenced by inductive effects, while the tetracyclic hapalindole formation (right side) is also influenced by resonance effects.

and Y101F_F138S). Our results provide further support that these residues are critical for the selectivity of the terminal reaction. For the Y101F and F138S mutants, we observed the coproduction of fischerindole and hapalindole products. However, upon screening the HpiC1 double mutant, we observed almost complete conversion to fischerindole metabolites. The F138S mutation also aided in uncovering the substrate selectivity differences between HpiC1 and FimC5, as product formation was either inhibited or completely abolished in select substrates. Exceptions to these results include compounds **13** and **17**, which displayed a 50:50 ratio of products for all mutants, and compound **18**, which led to formation of the tricyclic hapalindole **32** for all HpiC1 mutants tested (Table S37 and Figures S1−S11 in the Supporting Information).

Discovery and Isolation of Nitrile-Containing Compounds 30 and 40. Hapalindole-type indole alkaloids are noted for containing a rare isonitrile (−NC) moiety, although nitrile (−CN)-containing fischerindole and ambiguine molecules have been isolated previously.[1,3c,10] Derivation of the nitrile functionality from an isonitrile rearrangement has been suggested previously,[10] and we decided to examine this hypothesis by screening the Stig cyclases using *cis*-indole *nitrile* derivative **19**, which was accepted by the prenyltransferase FamD2 at a TTN value comparable to that of the native isonitrile compound (Table 2). A cyclized product from wild-type HpiC1 was not initially observed with **19**; however, the generation of two new products from each of the three HpiC1→FimC5 mutant cyclases in varying ratios was observed. Scale-up and structural characterization of products derived from the HpiC1 Y101F mutant led to identification of the 12-*epi*-hapalindole U nitrile derivative **30** (we also observed small amounts of the corresponding tricyclic hapalindole derivative). Wild-type HpiC1 and FamC1 were then rescreened under the optimized conditions (Experimental Section), resulting in the production of **30** for both enzymes. To our knowledge, these are the first nitrile-containing hapalindole molecules reported. With this result in hand, we returned to wild type FimC5 cyclase and, under the same optimized conditions, retested substrate **19**. We observed the production of the nitrile-containing 12-*epi*-fischerindole U derivative **40** that was inadvertently overlooked in our initial analysis. Thus, our results demonstrated that the FamC1, HpiC1, and FimC5 cyclases have the ability to catalyze cyclization of the isonitrile- and nitrile-containing indole subunits. However, the nitrile substrate appeared to have lower conversion and isolated yield values (Tables 3 and 4) in comparison to the native isonitrile substrate, suggesting that the nitrile moiety affects turnover from the 3-GC intermediate to the terminal tetracyclic product. Regardless, this result supports that the nitrile functionality may come from early modifications of the intermediates, but the source remains unknown.

Computational Analysis of the Reactivity of Substrates 17 and 18. To investigate why substrates **17** and **18** form tricyclic hapalindole compounds **31** and **32** with FamC1/HpiC1, respectively, while tetracyclic fischerindole **36** is formed with FimC5, we performed quantum mechanical density functional theory computations (Figure 3). For substrates **17** and **18**, as well as the parent indole intermediate **2**, we began with the tricyclic cationic intermediates **T** and considered two possible electrophilic aromatic substitutions: (1) reaction at C-4 to form the tetracyclic hapalindole scaffolds **H** and (2) reaction at C-2 to form the tetracyclic fischerindole

https://doi.org/10.1021/acscatal.0c05656
ACS Catal. 2021, 11, 4670−4681

scaffolds **F**. As shown in Figure 3, formation of hapalindole scaffolds is favored for the parent indole but disfavored for the azaindoles. The difference can be understood by a consideration of resonance structures that stabilize the hapalindole scaffold. While the conversion of indole cation **2-T** into **2-H** is exergonic by 1.9 kcal/mol and has a low free energy barrier of 7.4 kcal/mol, the conversion of azaindole cation **17-T** into **17-H** is endergonic by 10.0 kcal/mol and has a higher barrier of 14.7 kcal/mol. In particular, of the four resonance structures in addition to the iminium structure, the resonance structure shown places a positive charge on the electronegative nitrogen, resulting in less stabilization in comparison with the parent indole derivative, where this positive charge is on a carbon. The conversion of fluorinated azaindole cation **18-T** into **18-H** is only slightly more favorable due to near-cancellation of the resonance and inductive effects of **F**; this reaction is endergonic by 9.8 kcal/mol and has a barrier of 14.0 kcal/mol. Given the higher barriers to tetracyclic hapalindole formation for **17** and **18**, it is not surprising that FamC1 and HpiC1 fail to catalyze this reaction; instead, deprotonation of cations **17-T** and **18-T** yield tricyclic compounds **31** and **32**, respectively. Unlike the case for tetracyclic hapalindole formation, the conversion of azaindoles into tetracyclic fischerindole scaffolds does not exhibit differential resonance effects in comparison to the parent indole because the azaindole nitrogen and fluorine atoms are not on positively charged positions in any of the four additional resonance structures that stabilize each tetracyclic fischerindole scaffold. Instead, tetracyclic fischerindole formation is influenced by smaller inductive effects. Thus, the conversion of indole **2-T** into **2-F** is exergonic by 10.1 kcal/mol and the conversion of azaindole **17-T** into **17-F** (with an additional inductively withdrawing nitrogen atom) is exergonic by only 8.5 kcal/mol. The conversion of fluorinated azaindole **18-T** into **18-F**, which contains inductively withdrawing nitrogen and fluorine atoms, is exergonic by only 6.5 kcal/mol. The free energy barriers, which are 1.7, 1.9, and 2.9 kcal/mol, respectively, follow the same trend in which addition of inductively withdrawing atoms raises the transition-state energy. However, because these inductive effects are smaller than resonance effects, FimC5 can efficiently catalyze the conversion of **17** into **36**. Although it is important to note that these reactions take place in an enzyme active site, these computations addressing the innate reactivity of azaindoles reveal that tetracyclic hapalindole formation has a substantially higher free energy barrier in comparison to tetracyclic fischerindole formation. Accordingly, it is not surprising that FimC5 catalyzes tetracyclic fischerindole formation while FamC1 and HpiC1 form tricyclic products rather than tetracyclic hapalindoles. Evidently, the enzyme active sites do not overcome the innate difference in ease of tetracyclic product formation.

Analysis of Stig Cyclase Biocatalytic Ability. In this work, we explored the biocatalytic versatility of select Stig cyclases by assessing their substrate scope and ability to generate new derivatives. We analyzed HpiC1, select FamC1, and FimC5 reactions at both 2 and 5 mg scales to assess how scalability may affect the overall yield, which ranged from 10 to 60% (Tables 3 and 4) for both reactions. The isolated yields of certain substrates (**22** and **26** for HpiC1 and **39** for FimC5) were coincident with, or exceeded, the levels of the native substrate, suggesting that certain substituents enhance cyclase reactivity. In the majority of cases though, the isolated yields appeared to be significantly lower than the percent conversion values observed in the analytical-scale reactions. We believe that, through the filtration, workup, and purification process, a significant amount of material was lost and optimizing isolation methods may be necessary to address this issue. At the 5 mg scale with HpiC1, we observed that the tricyclic minor product was generated in a higher ratio in comparison to those for the 2 mg or analytical reactions. While these two compounds are separable, further scalability represents an objective for protein engineering to maximize tetracycle formation. However, FamC1 did show lower production of the tricyclic product but appears to be less efficient and flexible in comparison to HpiC1.

CONCLUSION

Through this work, we have shown the biocatalytic potential of core biosynthetic enzymes to produce unnatural hapalindole and fischerindole derivatives. The three cyclases investigated for this work, FamC1, HpiC1, and FimC5, along with select mutants and FamD2 geranyltransferase have demonstrated their ability to accept numerous unnatural *cis*-indole isonitrile (and nitrile) derivatives. These new compounds are poised for an investigation of biological activity by direct means or for additional semisynthetic or biocatalytic modifications. While HpiC1 appears to be the most versatile Stig cyclase, there are numerous additional homologues and heteromeric combinations that can be screened to further probe the full scope of Stig cyclase biocatalytic versatility. This work further supports the growing opportunity to employ natural product biosynthetic enzymes for the assembly of complex, bioactive small molecules and as a complement to synthetic chemistry approaches.

EXPERIMENTAL SECTION

General Considerations. All NMR spectra were acquired on a Varian 400 and 600 MHz and Bruker 800 MHz spectrometers. Proton and carbon signals are reported in parts per million (δ) using residual solvent signals as an internal standard. Analytical HPLC analysis was performed on a Shimadzu 2010 EV APCI spectrometer equipped with an LUNA C18 250 × 4.6 mm column, with a mobile phase gradient of 70−100% acetonitrile in water over 16 min at 40 °C, and was monitored by UV absorption at 280 nm. LC-MS analysis was performed on a Agilent Infinity II TOF instrument using an XBridge C18 2.1 × 150 mm column, with a mobile phase gradient of 70−100% acetonitrile in water over 12 min. Preparative-scale HPLC was performed on a Shimadzu 20-AT instrument equipped with an LUNA C18 250 × 10 mm column for 2 mg reactions and an LUNA C8 250 × 21 mm column for 5 mg reactions, with a mobile phase gradient of 50−100% or 60−100% acetonitrile in water over 60 min. Optical rotations were obtained using a Jasco P2000 polarimeter at 25 °C.

Escherichia coli strain BL21(DE3) was used for protein expression. Plasmid pET28H8T[8g] was used for cloning and expression of N-truncated FamC1 and FimC5. Plasmid pET28a was used for cloning and expression of FamD2, HpiC1, and HpiC1 mutants. Isopropyl β-D-thiogalactopyranoside (IPTG) was used to induce expression; DNase and lysozyme were purchased form Sigma-Aldrich. Ni-NTA agarose from Invitrogen was used to purify His-tag proteins.

All chemicals were purchased from Sigma-Aldrich, ACROS, and Combi-Blocks. Multiplicities are abbreviated as follows:

https://doi.org/10.1021/acscatal.0c05656
ACS Catal. 2021, 11, 4670−4681

singlet (s), doublet (d), triplet (t), quartet (q), doublet of doublets (dd), triplet of doublets (td), doublet of doublets of doublets (ddd), triplet of doublets of doublets (tdd), and multiplet (m). Chemical abbreviations are as follows: ethyl acetate (EtOAc), dichloromethane (DCM), tetrahydrofuran (THF), potassium bis(trimethylsilyl)amide (KHMDS), acetic acid (AcOH), sodium sulfate (Na_2SO_4), diethyl ether (Et_2O), phosphorus oxychloride ($POCl_3$), sodium hydroxide (NaOH), acetonitrile (CH_3CN), magnesium chloride ($MgCl_2$), calcium chloride ($CaCl_2$), and sodium chloride (NaCl).

Protein Expression and Purification. The expression and purification of proteins were performed as described.[8g,9] Briefly, a single BL21(DE3) colony was inoculated in LB medium containing 50 μg/mL of kanamycin and grown overnight at 37 °C with shaking at 200 rpm. The main culture (1 L) was inoculated at a dilution of 1:100 in a 2.8 L Fernbach flask containing TB medium and the same concentration of antibiotic. The cells were grown (37 °C, 200 rpm) to an optical density (A_{600} nm) of 1.0. The culture flasks were chilled in ice, the contents were induced with IPTG (0.2 mM), and the flasks were further incubated (18 °C, 200 rpm) for 16 h. The cells were harvested (5000 rpm, 4 °C, 15 min), flash-frozen, and stored at −80 °C until purification. The cell pellets were resuspended at 4 °C in the lysis buffer (10 mM HEPES, 50 mM NaCl, 0.2 mM TCEP, 10% glycerol, 20 mM imidazole), containing 0.5 mg/mL of lysozyme, 1 mM PMSF, and 1 mL of 2 mg/mL DNase. The mixture was stirred for 30 min and sonicated on ice for a total time of 120 s using 10 s pulses followed by a 50 s pause. The cellular debris was removed by centrifugation (65000*g*, 4 °C, 35 min). The clarified lysate was loaded onto Ni-NTA agarose column equilibrated with lysis buffer. The column was washed with two column volumes of wash buffer (10 mM HEPES, 300 mM NaCl, 0.2 mM TCEP, 10% glycerol, 20 mM imidazole) and the His-tagged protein was eluted with elution buffer (10 mM HEPES, 50 mM NaCl, 0.2 mM TCEP, 10% glycerol, 300 mM imidazole). The fractions were pooled and dialyzed overnight or by using a PD10-desalting column (GE Healthcare) with storage buffer (10 mM HEPES, 50 mM NaCl, 0.2 mM TCEP, 10% glycerol). The purified protein was analyzed by SDS-PAGE gel for purity, measured by Nanodrop using a calculated molar extinction coefficient for concentration, and flash-frozen in liquid nitrogen for storage at −80 °C.

Analytical, TTN, and Scale-Up Enzymatic Reactions. *cis*-Indole isonitrile derivatives were synthesized as described below. For the initial assays, a 50 μL reaction mixture containing 10 μM FamD2, 15 μM cyclase, 1 mM substrate, 1 mM GPP, 5 mM $MgCl_2$, 50 mM Tris pH 7.8 buffer, and 5 mM $CaCl_2$ was incubated at 37 °C for 4 h. The reaction was quenched twice with a 3× volume of EtOAc. The organic layers were combined, dried, and redissolved in 100 μL of acetonitrile for LCMS and HPLC analysis. HPLC conversion values were determined by the area under the curve of the residual starting material and newly formed product. For later assays, a 100 μL reaction mixture containing 5 μM FamD2, 20 μM cyclase, 1 mM substrate, 1.5 mM GPP, 5 mM $MgCl_2$, 50 mM of Tris pH 7.0 buffer and 7.5 mM $CaCl_2$ was incubated, quenched, and analyzed as previously described. For FamD2 TTN assays, a 100 μL reaction mixture containing 1 μM FamD2, 2 mM substrate, 1.5 mM GPP, 5 mM $MgCl_2$, and 50 mM Glycine pH 10.0 buffer was incubated at 37 °C for 1 h. The reaction was quenched and analyzed as described previously. TTN values were determined by standard curve analysis for the starting material (Tables S3−S15 in the Supporting Information). For the structure analysis and isolated yield values of the enzymatic products, the reactions were scaled up to 2 and 5 mg of starting material (10 and 25 mL, respectively) and the reaction mixtures incubated at 37 °C overnight or until HPLC showed consumption of the starting material. The products were extracted with EtOAc and purified by preparative HPLC as described in General Considerations. All products were obtained as white solids. The purified compounds were concentrated, dissolved in C_6D_6, and analyzed using Varian 600 MHz and Bruker 800 MHz NMR spectrometers.

Chemical Synthesis of *cis*-Indole Isonitrile Derivatives. All derivatives were prepared using methods previously described.[8f,9] Briefly, in a 50 mL two-neck round-bottom flask purged with nitrogen at −78 °C (dry ice/acetone), diethyl (isocyanomethyl)phosphonate (0.37 mL, 2.26 mmol) (diethyl (cyanomethyl)phosphonate was used for the production of **19**) was diluted with THF (5 mL). KHMDS (1 M THF, 2.60 mL, 2.60 mmol) was added dropwise, and the reaction mixture was stirred at −78 °C for 15 min. In a separate 4 mL vial, an indole-3-carboxaldehyde derivative (1.13 mmol) was dissolved in THF (5 mL), and the resulting solution was added dropwise to the KHMDS solution at −78 °C. The resulting mixture was stirred at 0 °C (cryocool) overnight or until TLC showed consumption of the starting material. The resulting solution was quenched by the addition of AcOH (0.15 mL, 2.6 mmol) and concentrated. The resulting residue was diluted with EtOAc (20 mL), washed with 1 M aqueous potassium phosphate buffer (20 mL, pH 7) and brine, dried with Na_2SO_4, and concentrated to a residue. The residue was dissolved in EtOAc and purified by flash chromatography (24−100% pentane/Et_2O, SiO_2) to afford the title compound as reported below. Yields and spectral data are reported below.

*(Z)-5-(Benzyloxy)-3-(2-isocyanovinyl)-1H-indole (**6**).* Blue solid, 17 mg, 11%. ^{1}H NMR (400 MHz, acetone-d_6): δ 5.17 (s, 2H), 5.90 (d, J = 8.9 Hz, 1H), 6.90−6.99 (m, 2H), 7.32 (t, J = 7.3 Hz, 1H), 7.37−7.47 (m, 4H), 7.51 (d, J = 7.5 Hz, 2H), 8.14 (d, J = 2.7 Hz, 1H), 10.80 (s, 1H). ^{13}C NMR (151 MHz, acetone): δ 169.52, 154.15, 137.99, 130.84, 128.32, 127.70, 127.58, 127.55, 127.32, 124.44, 113.46, 112.60, 109.49, 101.38, 70.17.

*(Z)-3-(2-Isocyanovinyl)-1H-indole-5-carbonitrile (**7**).* Tan solid, 25 mg, 22%. ^{1}H NMR (400 MHz, acetone-d_6): δ 6.06 (d, J = 8.9 Hz, 1H), 7.06 (dt, J = 9.2, 4.7 Hz, 1H), 7.53 (dd, J = 8.5, 1.6 Hz, 1H), 7.71 (dd, J = 8.4, 0.8 Hz, 1H), 8.24−8.29 (m, 1H), 8.32 (s, 1H), 11.38 (s, 1H). ^{13}C NMR (101 MHz, acetone): δ 171.15, 138.20, 129.86, 127.72, 126.16, 124.72, 124.10, 120.80, 114.08, 111.07, 104.41

*(Z)-3-(2-Isocyanovinyl)-5-methoxy-1H-indole (**8**).* Red solid, 36 mg, 16%. ^{1}H NMR (400 MHz, acetone-d_6): δ 3.84 (s, 3H), 5.89 (d, J = 8.8 Hz, 1H), 6.87 (dd, J = 8.8, 2.4 Hz, 1H), 6.97 (d, J = 6.0 Hz, 1H), 7.30 (d, J = 2.4 Hz, 1H), 7.41 (d, J = 8.7 Hz, 1H), 8.07−8.15 (m, 1H), 10.77 (s, 1H). ^{13}C NMR (151 MHz, dmso): δ 169.82, 154.74, 130.64, 127.65, 127.49, 125.45, 124.09, 113.16, 113.00, 109.24, 100.54, 55.83.

*(Z)-3-(2-Isocyanovinyl)-6-methoxy-1H-indole (**9**).* Tan solid, 5 mg, 5%. ^{1}H NMR (599 MHz, acetone-d_6): δ 3.82 (s, 4H), 5.91 (d, J = 8.8 Hz, 1H), 6.82 (dd, J = 8.7, 2.3 Hz, 1H), 6.93 (dt, J = 9.8, 4.8 Hz, 1H), 7.04 (d, J = 2.3 Hz, 1H), 7.64 (d, J = 8.7 Hz, 1H), 8.03 (d, J = 2.3 Hz, 1H), 10.67 (s, 1H). ^{13}C NMR (151 MHz, dmso): δ 169.84, 156.73, 136.44, 125.96, 125.32, 124.46, 123.68, 119.32, 110.83, 109.34, 95.19, 55.67.

https://doi.org/10.1021/acscatal.0c05656
ACS Catal. 2021, 11, 4670−4681

*(Z)-5-Chloro-3-(2-isocyanovinyl)-1H-indole (**10**).* Tan solid, 20 mg, 11%. ^{1}H NMR (400 MHz, acetone-d_6): δ 5.98 (d, J = 8.9 Hz, 1H), 6.93−7.06 (m, 0H), 7.22 (dd, J = 8.6, 2.0 Hz, 1H), 7.55 (d, J = 8.6 Hz, 1H), 7.82 (d, J = 2.0 Hz, 1H), 8.22 (d, J = 2.0 Hz, 1H), 11.04 (s, 1H).

*(Z)-6-Chloro-3-(2-isocyanovinyl)-1H-indole (**11**).* Yellow solid, 36 mg, 16%. ^{1}H NMR (599 MHz, acetone-d_6): δ 5.96 (d, J = 8.9 Hz, 1H), 6.94 (dt, J = 9.5, 4.9 Hz, 1H), 7.16 (dd, J = 8.5, 1.9 Hz, 1H), 7.57 (d, J = 1.8 Hz, 1H), 7.75 (d, J = 8.5 Hz, 1H), 8.17−8.20 (m, 1H), 11.02 (s, 1H). ^{13}C NMR (151 MHz, acetone): δ 170.89, 137.02, 128.93, 128.64, 128.47, 126.68, 124.71, 121.72, 120.25, 112.65, 110.61.

*(Z)-5-Fluoro-3-(2-isocyanovinyl)-1H-indole (**12**).* Tan solid, 36.7 mg, 18%. ^{1}H NMR (400 MHz, acetone-d_6): δ 5.95 (d, J = 8.9 Hz, 1H), 6.94 (p, J = 4.8 Hz, 1H), 7.03 (td, J = 9.1, 2.5 Hz, 1H), 7.52 (td, J = 9.9, 3.5 Hz, 2H), 8.23 (s, 1H), 10.97 (s, 1H).

*(Z)-6-Fluoro-3-(2-isocyanovinyl)-1H-indole (**13**).* Tan solid, 48 mg, 23%. ^{1}H NMR (400 MHz, acetone-d_6): δ 5.97 (d, J = 8.9 Hz, 1H), 6.93−7.01 (m, 2H), 7.27 (dd, J = 9.7, 2.3 Hz, 1H), 7.77 (dd, J = 8.7, 5.2 Hz, 1H), 8.17 (s, 1H), 10.93 (s, 1H).

*(Z)-5-Bromo-3-(2-isocyanovinyl)-1H-indole (**14**).* Red solid, 51 mg, 18%. ^{1}H NMR (400 MHz, acetone-d_6): δ 5.96 (d, J = 8.9 Hz, 1H), 6.97 (dt, J = 9.2, 4.7 Hz, 1H), 7.33 (dd, J = 8.6, 1.9 Hz, 1H), 7.49 (d, J = 8.6 Hz, 1H), 7.95 (d, J = 1.8 Hz, 1H), 8.20 (d, J = 2.2 Hz, 1H), 11.08 (s, 1H). ^{13}C NMR (101 MHz, acetone): δ 170.77, 135.27, 129.69, 128.97, 128.80, 126.21, 124.63, 121.61, 114.62, 114.27, 110.11.

*(Z)-6-Bromo-3-(2-isocyanovinyl)-1H-indole (**15**).* Red solid, 63 mg, 23%. ^{1}H NMR (400 MHz, acetone-d_6): δ 5.98 (d, J = 8.9 Hz, 1H), 6.85−7.00 (m, 1H), 7.29 (dd, J = 8.5, 1.8 Hz, 1H), 7.67−7.76 (m, 2H), 8.18 (d, J = 1.9 Hz, 1H), 10.99 (s, 1H). ^{13}C NMR (151 MHz, acetone): δ 169.98, 136.50, 127.61, 126.03, 123.70, 123.38, 119.69, 115.57, 114.74, 109.70, 104.77.

*(Z)-5-Iodo-3-(2-isocyanovinyl)-1H-indole (**16**).* Red solid, 60 mg, 18%. ^{1}H NMR (400 MHz, acetone-d_6): δ 5.98 (d, J = 8.9 Hz, 1H), 7.00 (d, J = 9.0 Hz, 1H), 7.40 (d, J = 8.5 Hz, 1H), 7.51 (dd, J = 8.6, 1.7 Hz, 1H), 8.16 (d, J = 3.0 Hz, 2H), 11.03 (s, 1H). ^{13}C NMR (151 MHz, acetone): δ 169.93, 152.01, 134.82, 130.90, 129.54, 127.63, 127.06, 123.71, 114.15, 108.91, 83.50.

*(Z)-3-(2-Isocyanovinyl)-1H-pyrrolo[2,3-b]pyridine (**17**).* White solid, 26 mg, 13%. ^{1}H NMR (599 MHz, acetone-d_6): δ 1.70−1.84 (m, 0H), 3.56−3.66 (m, 0H), 6.01 (d, J = 8.9 Hz, 1H), 6.97 (dt, J = 9.8, 5.1 Hz, 1H), 7.20 (dd, J = 7.9, 4.7 Hz, 1H), 8.20 (dd, J = 7.9, 1.6 Hz, 1H), 8.26 (s, 1H), 8.35 (dd, J = 4.6, 1.6 Hz, 1H), 11.38 (s, 1H). ^{13}C NMR (151 MHz, acetone): δ 170.07, 148.22, 144.26, 127.05, 126.63, 123.64, 118.94, 116.61, 108.38, 105.03.

*(Z)-5-Fluoro-3-(2-isocyanovinyl)-1H-pyrrolo[2,3-b]-pyridine (**18**).* White solid, 38 mg, 18%. ^{1}H NMR (400 MHz, acetone-d_6): δ 6.04 (d, J = 8.9 Hz, 1H), 6.95 (dt, J = 9.5, 5.0 Hz, 1H), 8.04 (dd, J = 9.3, 2.7 Hz, 1H), 8.26 (t, J = 2.2 Hz, 1H), 8.33 (d, J = 2.1 Hz, 1H), 11.44 (s, 1H). ^{13}C NMR (151 MHz, acetone): δ 170.20, 156.91, 155.31, 144.88, 132.67, 132.48, 129.23, 123.38, 119.29, 119.25, 112.50, 112.35, 108.61.

*(Z)-3-(1H-indol-3-yl)acrylonitrile (**19**).* Yellow solid, 30 mg, 16%. ^{1}H NMR (400 MHz, acetone-d_6): δ 5.37 (dd, J = 11.8, 1.1 Hz, 1H), 7.14−7.31 (m, 2H), 7.50−7.60 (m, 1H), 7.67 (d, J = 11.7 Hz, 1H), 7.77−7.86 (m, 1H), 8.37 (s, 1H), 11.02 (s, 1H).

Chemical Synthesis of Indole-3-carboxaldehyde Derivatives. All derivatives were prepared using the same method. Briefly, in a 25 mL round-bottom flask purged with nitrogen at 0 °C (ice−water bath), $POCl_3$ (1.38 mL, 14.7 mmol) was stirred in dry DMF (4 mL) for 20 min. In a separate 4 mL vial, the reactant indole compound (2.94 mmol) was dissolved in dry DMF (4 mL) and added to the $POCl_3$ solution at 0 °C. The reaction mixture was slowly brought to room temperature and stirred for 1 h or until TLC showed consumption of the starting material. The reaction mixture was cooled to 0 °C and quenched with ice−water and 1 M NaOH (5 mL each). The reaction mixture was stirred at room temperature for 1 h or until TLC showed consumption of the intermediate. The resulting solution was extracted with EtOAc (2 × 10 mL), and the extract was washed with brine, dried with Na_2SO_4, and concentrated to a residue. The residue was dissolved in EtOAc and purified by flash chromatography (16−100% hexanes/EtOAc, SiO_2) to afford the title compound as reported below. Yields and spectral data are reported below.

*5-Iodo-1H-indole-3-carbaldehyde (**20**).* Off-white solid, 259 mg, 46%. ^{1}H NMR (400 MHz, acetone-d_6): δ 7.42 (dd, J = 8.5, 0.6 Hz, 1H), 7.58 (dd, J = 8.6, 1.8 Hz, 1H), 8.22 (s, 1H), 8.56−8.66 (m, 1H), 10.01 (s, 1H).

*5-Fluoro-1H-pyrrolo[2,3-b]pyridine-3-carbaldehyde (**21**).* White solid, 88 mg, 18%. ^{1}H NMR (400 MHz, acetone-d_6): δ 8.20 (dd, J = 8.8, 2.8 Hz, 1H), 8.31 (dd, J = 2.8, 1.8 Hz, 1H), 8.48 (s, 1H), 10.01 (s, 1H), 11.69 (s, 1H).

Chemical Synthesis of Geranyl Diphosphate Triammonium. Geranyl diphosphate was synthesized as described previously.[11] In a 10 mL round-bottom flask purged with nitrogen, tris(tetrabutylammonium) hydrogen pyrophosphate (1.0 g, 1.04 mmol) was dissolved in CH_3CN (1.0 mL). Geranyl chloride (0.09 mL, 0.475 mmol) was added, and the reaction mixture was stirred at room temperature for 2 h.

Dowex 50WX8 Resin Preparation. Dowex 50WX8 resin (20 g, hydrogen form) was washed with half-saturated aqueous ammonium chloride (5 × 50 mL) and water (5 × 50 mL) until the pH of the supernatant equaled 5. The slurry was rinsed twice with ion exchange buffer (2% isopropyl alcohol in 25 mM aqueous ammonium bicarbonate), loaded into a flash column, and equilibrated with ion exchange buffer.

Purification. The reaction mixture was concentrated to afford an orange residue that was diluted with ion exchange buffer. The crude mixture was chromatographed with two column volumes of ion exchange buffer (75 mL). The fractions were combined, concentrated by rotary evaporation, flash-frozen, and lyophilized for 2 days. The resulting white powder was diluted with 0.1 M ammonium bicarbonate (4 mL) and 50% isopropyl alcohol/CH_3CN (10 mL), vortexed for 30 s and centrifuged (2000 rpm, rt, 5 min). The organic layer was extracted, the residual 0.5 mL of yellow liquid was diluted with 50% isopropyl alcohol/CH_3CN and the dilution/vortex/centrifugation process was repeated twice. The combined organic layers were concentrated to afford a while solid. The white solid was taken up in 50% isopropyl alcohol/25% CH_3CN/25% 0.1 M aqueous ammonium bicarbonate and chromatographed with cellulose. The resulting fractions were combined and lyophilized, affording the title compound as a white powder (138 mg, 80.3%).

^{1}H NMR (400 MHz, D_2O/ND_4OD): δ 1.92 (d, J = 1.3 Hz, 3H), 1.98 (s, 3H), 2.01 (d, J = 1.3 Hz, 3H), 2.39 (d, J = 6.5 Hz, 2H), 2.41−2.49 (m, 2H), 5.45−5.53 (m, 1H), 5.74 (dt, J = 6.1, 3.9 Hz, 1H). ^{13}C NMR (151 MHz, D_2O/ND_4OD): δ

https://doi.org/10.1021/acscatal.0c05656
ACS Catal. 2021, 11, 4670−4681

142.46, 133.67, 124.40, 120.46, 62.61, 39.10, 25.92, 25.16, 17.26, 15.89. ^{31}P NMR (162 MHz, D_2O/ND_4OD): δ −9.93 (d, J = 21.6 Hz), −6.08 (d, J = 21.6 Hz).

Structure Determination. Colorless plates of **36** were grown from a diethyl ether/hexanes solution of the compound at 4 °C. A crystal of dimensions 0.06 × 0.04 × 0.02 mm was mounted on a Rigaku AFC10K Saturn 944+ CCD-based X-ray diffractometer equipped with a low-temperature device and a Micromax-007HF Cu-target microfocus rotating anode (λ = 1.54187 A) operated at 1.2 kW power (40 kV, 30 mA). The X-ray intensities were measured at 85(1) K with the detector placed at a distance 42.00 mm from the crystal. A total of 2028 images were collected with an oscillation width of 1.0° in ω. The exposure times were 5 s for the low-angle images and 45 s for the high angle images. Rigaku d*trek images were exported to CrysAlisPro for processing and corrected for absorption. The integration of the data yielded a total of 61153 reflections to a maximum 2θ value of 139.83°, 7384 of which were independent and 5502 were greater than $2\sigma(I)$. The final cell constants (Table S36) were based on the xyz centroids of 8462 reflections above $10\sigma(I)$. An analysis of the data showed negligible decay during the data collection. The structure was solved and refined with the Bruker SHELXTL (version 2018/3) software package, using the space group $P2_12_12_1$ with Z = 4 for the formula $C_{44}H_{56}N_6O$. All non-hydrogen atoms were refined anisotropically with the hydrogen atoms placed in a combination of idealized and refined positions. Full-matrix least-squares refinement based on F^2 converged at R1 = 0.0885 and wR2 = 0.2349 (for $I > 2\sigma(I)$) and R1 = 0.1102 and wR2 = 0.2582 for all data. Additional details are presented in Tables S38−S44 and are given in the Supporting Information.

■ ASSOCIATED CONTENT

Supporting Information

The Supporting Information is available free of charge at https://pubs.acs.org/doi/10.1021/acscatal.0c05656.

Full amino acid sequences, mutagenic primers, TTN tables, compound characterization tables, mutagenesis percent conversion tables, mutagenesis HPLC traces, NMR spectra, MS traces, crystallographic data and parameters, and computational methods (PDF)

Crystallographic data for **36** (CIF)

■ AUTHOR INFORMATION

Corresponding Author

David H. Sherman − *Life Sciences Institute, Department of Medicinal Chemistry, and Department of Microbiology & Immunology, Department of Chemistry, University of Michigan, Ann Arbor, Michigan 48109-2216, United States;* orcid.org/0000-0001-8334-3647; Email: davidhs@umich.edu

Authors

Robert M. Hohlman − *Life Sciences Institute and Department of Medicinal Chemistry, University of Michigan, Ann Arbor, Michigan 48109-2216, United States;* orcid.org/0000-0002-0361-1611

Sean A. Newmister − *Life Sciences Institute, University of Michigan, Ann Arbor, Michigan 48109-2216, United States*

Jacob N. Sanders − *Department of Chemistry and Biochemistry, University of California, Los Angeles, Los Angeles, California 90095, United States;* orcid.org/0000-0002-2196-4234

Yogan Khatri − *Life Sciences Institute, University of Michigan, Ann Arbor, Michigan 48109-2216, United States;* orcid.org/0000-0002-2432-7679

Shasha Li − *Life Sciences Institute and Department of Medicinal Chemistry, University of Michigan, Ann Arbor, Michigan 48109-2216, United States*

Nikki R. Keramati − *Life Sciences Institute, University of Michigan, Ann Arbor, Michigan 48109-2216, United States*

Andrew N. Lowell − *Life Sciences Institute, University of Michigan, Ann Arbor, Michigan 48109-2216, United States;* orcid.org/0000-0001-5357-5279

K. N. Houk − *Department of Chemistry and Biochemistry, University of California, Los Angeles, Los Angeles, California 90095, United States;* orcid.org/0000-0002-8387-5261

Complete contact information is available at: https://pubs.acs.org/10.1021/acscatal.0c05656

Author Contributions

R.M.H., A.N.L., and D.H.S. designed the research. R.M.H. and N.R.K. performed all experiments and characterized all compounds. S.A.N. and Y.K. aided in the expression and purification of all proteins. J.N.S. performed quantum mechanical computations, and J.N.S. and K.N.H. wrote the computational section of the manuscript. S.L. cloned the expression plasmids for FamD2, FamC1, HpiC1, and FimC5. A.N.L. and R.M.H. synthesized unnatural *cis*-indole isonitrile substrates. R.M.H., S.A.N., and D.H.S. contributed to the preparation of the manuscript.

Notes

The authors declare no competing financial interest.

■ ACKNOWLEDGMENTS

We are grateful to the National Science Foundation under the CCI Center for Selective C−H Functionalization (CHE-1700982), National Institutes of Health (R35 GM118101), and the Hans W. Vahlteich Professorship (to D.H.S.) and ACS MEDI Pre-Doctoral Fellowship (to R.M.H) for financial support. J.N.S. acknowledges support from the National Institute of General Medical Sciences of the National Institutes of Health (F32 GM122218). The authors thank Dr. Jeffery Kampf (University of Michigan Department of Chemistry) for X-ray crystallographic work and Dr. Pavel Nagorny for access to their polarimeter. Funding from NSF grant CHE-0840456 helped defray costs of small molecule X-ray instrumentation. Computational resources were provided by the UCLA Institute for Digital Research and Education (IDRE) and by the San Diego Supercomputing Center (SDSC) through XSEDE (ACI-1548562).

■ REFERENCES

(1) Walton, K.; Berry, J. P. Indole Alkaloids of the Stigonematales (Cyanophyta): Chemical Diversity, Biosynthesis and Biological Activity. *Mar. Drugs* **2016**, *14*, 73.

(2) Bhat, V.; Dave, A.; MacKay, J. A.; Rawal, V. H. The Chemistry of Hapalindoles, Fischerindoles, Ambiguines, and Welwitindolinones. In *The Alkaloids: Chemistry and Biology*; Academic Press: New York, 2014; Vol. 73, Chapter 2, pp 65−160.

(3) (a) Mo, S.; Krunic, A.; Chlipala, G.; Orjala, J. Antimicrobial Ambiguine Isonitriles from the Cyanobacterium *Fischerella ambigua*. *J. Nat. Prod.* **2009**, *72*, 894−899. (b) Mo, S.; Krunic, A.; Santarsiero, B. D.; Franzblau, S. G.; Orjala, J. Hapalindole-related alkaloids from the

cultured cyanobacterium *Fischerella ambigua*. *Phytochemistry* **2010**, *71*, 2116−2123. (c) Kim, H.; Lantivit, D.; Hwang, C. H.; Kroll, D. J.; Swanson, S. M.; Franzblau, S. G.; Orjala, J. Indole alkaloids from two cultured cyanobacteria, *Westiellopsis* sp. and *Fischerella muscicola*. *Bioorg. Med. Chem.* **2012**, *20*, 5290−5295. (d) Raveh, A.; Carmeli, S. Antimicrobial Ambiguines from the Cyanobacterium *Fischerella* sp. Collected in Israel. *J. Nat. Prod.* **2007**, *70*, 196−201. (e) Moore, R. E.; Cheuk, C.; Yang, X. Q. G.; Patterson, G. M. L.; Bonjouklian, R.; Smitka, T. A.; Mynderse, J. S.; Foster, R. S.; Jones, N. D.; Swartzendruber, J. K.; Deeter, J. B. Hapalindoles, antibacterial and antimycotic alkaloids from the cyanophyte *Hapalosiphon fontinalis*. *J. Org. Chem.* **1987**, *52*, 1036−1043. (f) Asthana, R. K.; Srivastava, A.; Singh, A. P.; Deepali; Singh, S. P.; Nath, G.; Srivastava, R.; Srivastava, B. S. Identification of an antimicrobial entity from the cyanobacterium *Fischerella* sp. isolated from bark of *Azadirachta indica* (Neem) tree. *J. Appl. Phycol.* **2006**, *18*, 33−39.

(4) Smitka, T. A.; Bonjouklian, R.; Doolin, L.; Jones, N. D.; Deeter, J. B.; Yoshida, W. Y.; Prinsep, M. R.; Moore, R. E.; Patterson, G. M. L. Ambiguine isonitriles, fungicidal hapalindole-type alkaloids from three genera of blue-green algae belonging to the Stigonemataceae. *J. Org. Chem.* **1992**, *57*, 857−861.

(5) (a) Stratmann, K.; Moore, R. E.; Bonjouklian, R.; Deeter, J. B.; Patterson, G. M. L.; Shaffer, S.; Smith, C. D.; Smitka, T. A. Welwitindolinones, Unusual Alkaloids from the Blue-Green Algae *Hapalosiphon welwitschii* and *Westiella intricata*. Relationship to Fischerindoles and Hapalinodoles. *J. Am. Chem. Soc.* **1994**, *116*, 9935−9942. (b) Smith, C. D.; Zilfou, J. T.; Stratmann, K.; Patterson, G. M. L.; Moore, R. E. Welwitindolinone analogues that reverse P-glycoprotein-mediated multiple drug resistance. *Mol. Pharmacol.* **1995**, *47*, 241−247. (c) Zhang, X.; Smith, C. D. Microtubule effects of welwistatin, a cyanobacterial indolinone that circumvents multiple drug resistance. *Mol. Pharmacol.* **1996**, *49*, 288−294.

(6) Chilczuk, T.; Steinborn, C.; Breinlinger, S.; Zimmermann-Klemd, A. M.; Huber, R.; Enke, H.; Enke, D.; Niedermeyer, T. H. J.; Grundemann, C. Hapalindoles from the Cyanobacterium *Hapalosiphon* sp. Inhibit T Cell Proliferation. *Planta Med.* **2020**, *86*, 96−103.

(7) (a) Dethe, D. H.; Das, S.; Kumar, V. B.; Mir, N. A. Enantiospecific Total Syntheses of (+)-Hapalindole H and (−)-12-*epi*-Hapalindole U. *Chem. Eur. J.* **2018**, *24*, 8980−8984. (b) Richter, J. M.; Ishihara, Y.; Masuda, T.; Whitefield, B. W.; Llamas, T.; Pohjakallio, A.; Baran, P. S. Enantiospecific Total Synthesis of the Hapalindoles, Fischerindoles, and Welwitindolinones *via* a Redox Economic Approach. *J. Am. Chem. Soc.* **2008**, *130*, 17938−17954. (c) Rafferty, R. J.; Williams, R. M. Formal Synthesis of Hapalindole O and Synthetic Efforts towards Hapalindole K and Ambiguine A. *Heterocycles* **2012**, *86*, 219−231. (d) Connon, R.; Guiry, P. J. Recent advances in the development of one-pot/multistep syntheses of 3,4-annulated indoles. *Tetrahedron Lett.* **2020**, *61*, 151696. (e) Maimone, T. J.; Ishihara, Y.; Baran, P. S. Scalable total syntheses of (−)-hapalindole U and (+)-ambiguine H. *Tetrahedron* **2015**, *71*, 3652−3665. (f) Fukuyama, T.; Chen, X. Stereocontrolled Synthesis of (−)-Hapalindole G. *J. Am. Chem. Soc.* **1994**, *116*, 3125−3126. (g) Sahu, S.; Das, B.; Maji, M. S. Stereodivergent Total Synthesis of Hapalindoles, Fischerindoles, Hapalonamide H, and Ambiguine H Alkaloids by Developing a Biomimetic, Redox-Neutral, Cascade Prins-Type Cyclization. *Org. Lett.* **2018**, *20*, 6485−6489. (h) Vaillancourt, V.; Albizati, K. F. Synthesis and absolute configuration of (+)-hapalindole Q. *J. Am. Chem. Soc.* **1993**, *115*, 3499−3502. (i) Kinsman, A. C.; Kerr, M. A. The Total Synthesis of (+)-Hapalindole Q by an Organomediated Diels−Alder Reaction. *J. Am. Chem. Soc.* **2003**, *125*, 14120−14125. (j) Kinsman, A. C.; Kerr, M. A. Total Synthesis of (±)-Hapalindole Q. *Org. Lett.* **2001**, *3*, 3189−3191. (k) Bhat, V.; Allan, K. M.; Rawal, V. H. Total Synthesis of *N* -Methylwelwitindolinone D Isonitrile. *J. Am. Chem. Soc.* **2011**, *133*, 5798−5801. (l) Gademann, K.; Bonazzi, S. Total Synthesis of Complex Cyanobacterial Alkaloids without Using Protecting Groups. *Angew. Chem. Int. Ed.* **2007**, *46*, 5656−5658. (m) Lu, Z.; Yang, M.; Chen, P.; Xiong, X.; Li, A. Total Synthesis of Hapalindole-Type Natural Products. *Angew. Chem. Int. Ed.* **2014**, *53*, 13840−13844. (n) Rafferty, R. J.; Williams, R. M. Total Synthesis of Hapalindoles J and U. *J. Org. Chem.* **2012**, *77*, 519−524. (o) Baran, P. S.; Maimone, T. J.; Richter, J. M. Total synthesis of marine natural products without using protecting groups. *Nature* **2007**, *446*, 404−408. (p) Johnson, R. E.; Ree, H.; Hartmann, M.; Lang, L.; Sawano, S.; Sarpong, R. Total Synthesis of Pentacyclic (−)-Ambiguine P Using Sequential Indole Functionalizations. *J. Am. Chem. Soc.* **2019**, *141*, 2233−2237. (q) Xu, J.; Rawal, V. H. Total Synthesis of (−)-Ambiguine P. *J. Am. Chem. Soc.* **2019**, *141*, 4820−4823. (r) Chandra, A.; Johnston, J. N. Total Synthesis of the Chlorine-Containing Hapalindoles K, A, and G. *Angew. Chem. Int. Ed.* **2011**, *50*, 7641−7644. (s) Reisman, S. E.; Ready, J. M.; Hasuoka, A.; Smith, C. J.; Wood, J. L. Total Synthesis of (±)-Welwitindolinone A Isonitrile. *J. Am. Chem. Soc.* **2006**, *128*, 1448−1449. (t) Baran, P. S.; Richter, J. M. Direct Coupling of Indoles with Carbonyl Compounds: Short, Enantioselective, Gram-Scale Synthetic Entry into the Hapalindole and Fischerindole Alkaloid Families. *J. Am. Chem. Soc.* **2004**, *126*, 7450−7451. (u) Muratake, H.; Natsume, M. Total synthesis of marine alkaloids (±)-hapalindoles J and M. *Tetrahedron Lett.* **1989**, *30*, 1815−1818. (v) Muratake, H.; Natsume, M. Synthetic studies of marine alkaloids hapalindoles. Part 2. Lithium aluminum hydride reduction of the electron-rich carbon-carbon double bond conjugated with the indole nucleus. *Tetrahedron* **1990**, *46*, 6343−6350. (w) Muratake, H.; Kumagami, H.; Natsume, M. Synthetic studies of marine alkaloids hapalindoles. Part 3 Total synthesis of (±)-hapalindoles H and U. *Tetrahedron* **1990**, *46*, 6351−6360. (x) Bhat, V.; Allan, K. M.; Rawal, V. H. Total Synthesis of *N*-Methylwelwitindolinone D Isonitrile. *J. Am. Chem. Soc.* **2011**, *133*, 5798−5801. (y) Weires, N. A.; Styduhar, E. D.; Baker, E. L.; Garg, N. K. Total Synthesis of (−)-*N*-Methylwelwitindolinone B Isothiocyanate via a Chlorinative Oxabicycle Ring-Opening Strategy. *J. Am. Chem. Soc.* **2014**, *136*, 14710−14713. (z) Styduhar, E. D.; Huters, A. D.; Weires, N. A.; Garg, N. K. Enantiospecific Total Synthesis of *N*-Methylwelwitindolinone D Isonitrile. *Angew. Chem. Int. Ed.* **2013**, *52*, 12422−12425. (aa) Quasdorf, K. W.; Huters, A. D.; Lodewyk, M. W.; Tantillo, D. J.; Garg, N. K. Total Synthesis of Oxidized Welwitindolinones and (−)-*N*-Methylwelwitindolinone C Isonitrile. *J. Am. Chem. Soc.* **2012**, *134*, 1396−1399. (ab) Huters, A. D.; Styduhar, E. D.; Garg, N. K. Total Syntheses of the Elusive Welwitindolinones with Bicyclo[4.3.1] Cores. *Angew. Chem. Int. Ed.* **2012**, *51*, 3758−3765. (ac) MacKay, J. A.; Bishop, R. L.; Rawal, V. H. Rapid Synthesis of the *N*-Methylwelwitindolinone Skeleton. *Org. Lett.* **2005**, *7*, 3421−3424. (ad) Bhat, V.; Rawal, V. H. Stereocontrolled Synthesis of 20,21-Dihydro *N*-Methylwelwitindolinone B Isothiocyanate. *Chem. Commun.* **2011**, *47*, 9705−9707. (ae) Bhat, V.; MacKay, J. A.; Rawal, V. H. Lessons Learned While Traversing the Welwitindolinone Alkaloids Obstacle Course. *Tetrahedron* **2011**, *67*, 10097−10104. (af) Bhat, V.; MacKay, J. A.; Rawal, V. H. Directed Oxidative Cyclizations to C2- or C4-Positions of Indole: Efficient Construction of the Bicyclo[4.3.1]Decane Core of Welwitindolinones. *Org. Lett.* **2011**, *13*, 3214−3217. (ag) Allan, K. M.; Kobayashi, K.; Rawal, V. H. A Unified Route to the Welwitindolinone Alkaloids: Total Syntheses of (−)-*N*-Methylwelwitindolinone C Isothiocyanate, (−)-*N*-Methylwelwitindolinone C Isonitrile, and (−)-3-Hydroxy-*N*-Methylwelwitindolinone C Isothiocyanate. *J. Am. Chem. Soc.* **2012**, *134*, 1392−1395.

(8) (a) Hillwig, M. L.; Zhu, Q.; Liu, X. Biosynthesis of Ambiguine Indole Alkaloids in Cyanobacterium *Fischerella ambigua*. *ACS Chem. Biol.* **2014**, *9*, 372−377. (b) Chang, W. C.; Sanyal, D.; Huang, J. L.; Ittiamornkul, K.; Zhu, Q.; Liu, X. In Vitro Stepwise Reconstitution of Amino Acid Derived Vinyl Isocyanide Biosynthesis: Detection of an Elusive Intermediate. *Org. Lett.* **2017**, *19*, 1208−1211. (c) Ittiamornkul, K.; Zhu, Q.; Gkotsi, D. S.; Smith, D. M. R.; Hillwig, M. L.; Nightingale, N.; Goss, R. J. M.; Liu, X. Promiscuous indolyl vinyl isonitrile synthases in the biogenesis and diversification of hapalindole-type alkaloids. *Chem. Sci.* **2015**, *6*, 6836−6840. (d) Liu, X.; Hillwig, M. L.; Koharudin, L. M. I.; Gronenborn, A. M. Unified biogenesis of ambiguine, fischerindole, hapalindole and welwitindolinone: identification of a monogeranylated indolenine as a cryptic common biosynthetic intermediate by an unusual magnesium-

https://doi.org/10.1021/acscatal.0c05656
ACS Catal. 2021, 11, 4670−4681

dependent aromatic prenyltransferase. *Chem. Commun.* **2016**, *52*, 1737−1740. (e) Hillwig, M. L.; Fuhrman, H. A.; Ittiamornkul, K.; Sevco, T. J.; Kwak, D. H.; Liu, X. Identification and Characterization of a Welwitindolinone Alkaloid Biosynthetic Gene Cluster in the Stigonematalean Cyanobacterium *Hapalosiphon welwitschii*. *ChemBioChem* **2014**, *15*, 665−669. (f) Li, S.; Lowell, A. N.; Yu, F.; Raveh, A.; Newmister, S. A.; Bair, N.; Schaub, J. M.; Williams, R. M.; Sherman, D. H. Hapalindole/Ambiguine Biogenesis Is Mediated by a Cope Rearrangement, C−C Bond-Forming Cascade. *J. Am. Chem. Soc.* **2015**, *137*, 15366−15369. (g) Li, S.; Lowell, A. N.; Newmister, S. A.; Yu, F.; Williams, R. M.; Sherman, D. H. Decoding cyclase-dependent assembly of hapalindole and fischerindole alkaloids. *Nat. Chem. Biol.* **2017**, *13*, 467−469. (h) Newmister, S. A.; Li, S.; Garcia-Borras, M.; Sanders, J. N.; Yang, S.; Lowell, A. N.; Yu, F.; Smith, J. L.; Williams, R. M.; Houk, K. N.; Sherman, D. H. Structural basis of the Cope rearrangement and cyclization in hapalindole biogenesis. *Nat. Chem. Biol.* **2018**, *14*, 345−351. (i) Li, S.; Newmister, S. A.; Lowell, A. N.; Zi, J.; Chappell, C. R.; Yu, F.; Hohlman, R. M.; Orjala, J.; Williams, R. M.; Sherman, D. H. Control of Stereoselectivity in Diverse Hapalindole Metabolites is Mediated by Cofactor-Induced Combinatorial Pairing of Stig Cyclases. *Angew. Chem. Int. Ed.* **2020**, *59*, 8166−8172. (j) Micallef, M. L.; Sharma, D.; Bunn, B. M.; Gerwick, L.; Viswanathan, R.; Moffitt, M. C. Comparative analysis of hapalindole, ambiguine and welwitindolinone gene clusters and reconstitution of indole-isonitrile biosynthesis from cyanobacteria. *BMC Microbiol.* **2014**, *14*, 213. (k) Yu, C. P.; Tang, Y.; Cha, L.; Milikisiyants, S.; Smirnova, T. I.; Smirnov, A. I.; Guo, Y.; Chang, W. C. Elucidating the Reaction Pathway of Decarboxylation-Assisted Olefination Catalyzed by a Mononuclear Non-Heme Iron Enzyme. *J. Am. Chem. Soc.* **2018**, *140*, 15190−15193. (l) Bornemann, V.; Patterson, G. M. L.; Moore, R. E. Isonitrile biosynthesis in the cyanophyte *Hapalosiphon fontinalis*. *J. Am. Chem. Soc.* **1988**, *110*, 2339−2340. (m) Harris, N. C.; Born, D. A.; Cai, W.; Huang, Y.; Martin, J.; Khalaf, R.; Drennan, C. L.; Zhang, W. Isonitrile Formation by a Non-Heme Iron(II)-Dependent Oxidase/Decarboxylase. *Angew. Chem. Int. Ed.* **2018**, *130*, 9855−9858. (n) Awakawa, T.; Mori, T.; Nakashima, Y.; Zhai, R.; Wong, C. P.; Hillwig, M. L.; Liu, X.; Abe, I. Molecular Insight into the Mg2+-Dependent Allosteric Control of Indole Prenylation by Aromatic Prenyltransferase AmbP1. *Angew. Chem. Int. Ed.* **2018**, *57*, 6810−6813. (o) Wang, J.; Chen, C. C.; Yang, Y.; Liu, W.; Ko, T. P.; Shang, N.; Hu, X.; Xie, Y.; Huang, J. W.; Zhang, Y.; Guo, R. T. Structural insight into a novel indole prenyltransferase in hapalindole-type alkaloid biosynthesis. *Biochem. Biophys. Res. Commun.* **2018**, *495*, 1782−1788. (p) Chen, C. C.; Hu, X.; Tang, X.; Yang, Y.; Ko, T. P.; Gao, J.; Zheng, Y.; Huang, J. W.; Yu, Z.; Li, L.; Han, S.; Cai, N.; Zhang, Y.; Liu, W.; Guo, R. T. The Crystal Structure of a Class of Cyclases that Catalyze the Cope Rearrangement. *Angew. Chem. Int. Ed.* **2018**, *57*, 15060−15064. (q) Wong, C. P.; Awakawa, T.; Nakashima, Y.; Mori, T.; Zhu, Q.; Liu, X.; Abe, I. Two Distinct Substrate Binding Modes for the Normal and Reverse Prenylation of Hapalindoles by the Prenyltransferase AmbP3. *Angew. Chem. Int. Ed.* **2018**, *57*, 560−563. (r) Hillwig, M. L.; Liu, X. A new family of iron-dependent halogenases act on freestanding substrates. *Nat. Chem. Biol.* **2014**, *10*, 921−923. (s) Zhu, Q.; Liu, X. Discovery of a Calcium-Dependent Enzymatic Cascade for the Selective Assembly of Hapalindole-Type Alkaloids: On the Biosynthetic Origin of Hapalindole U. *Angew. Chem. Int. Ed.* **2017**, *56*, 9062−9066. (t) Zhu, Q.; Liu, X. Molecular and genetic basis for early stage structural diversifications in hapalindole-type alkaloid biogenesis. *Chem. Commun.* **2017**, *53*, 2826−2829.

(9) Khatri, Y.; Hohlman, R. M.; Mendoza, J.; Li, S.; Lowell, A. N.; Asahara, H.; Sherman, D. H. Multicomponent Microscale Biosynthesis of Unnatural Cyanobacterial Indole Alkaloids. *ACS Synth. Biol.* **2020**, *9*, 1349−1360.

(10) Huber, U.; Moore, R. E.; Patterson, G. M. L. Isolation of a Nitrile-Containing Indole Alkaloid from the Terrestrial Blue-Green Alga *Hapalosiphon delicatulus*. *J. Nat. Prod.* **1998**, *61*, 1304−1306.

(11) Davisson, V. J.; Woodside, A. B.; Neal, T. R.; Stremler, K. E.; Muehlbacher, M.; Poulter, C. D. Phosphorylation of isoprenoid alcohols. *J. Org. Chem.* **1986**, *51*, 4768−4779.

https://doi.org/10.1021/acscatal.0c05656
ACS Catal. 2021, 11, 4670−4681